EXPERIMENTAL INVESTIGATION OF WALL-PRESSURE FLUCTUATIONS ON A TRANSIENTLY MOVING HYDROFOIL

ÉTUDE EXPÉRIMENTALE DU CHAMP DE PRESSION PARIÉTALE SUR UN HYDROFOIL EN MOUVEMENT FORCÉ TRANSITOIRE

S. BENRAMDANE, J. A. ASTOLFI, J. -C. CEXUS, A. BOUDRAA

IRENav, EA 3634, École navale, BP600, 29240 Brest Armées

Résumé

Ce travail présente une étude expérimentale du champ de pression pariétale sur un corps portant en mouvement de rotation transitoire de grande amplitude. Les signaux obtenus sont instationnaires, turbulent, large bande, bruités et incluent différentes caractéristiques de l'écoulement apparaissant au cours du mouvement transitoire. Dans ce cadre l'analyse des signaux de pression a été réalisée à l'aide d'une technique de décomposition modale empirique (EMD) adaptée aux signaux transitoires qui décompose le signal en bandes de fréquences sur la base de fonctions modales intrinsèques (IMFs). La méthode sépare ainsi les composantes hautes fréquences des composantes basses fréquences intrinsèques au signal étudié. Outre le bruit haute fréquence elle permet de distinguer un certain nombre de caractéristiques de l'écoulement comme la transition laminaire-turbulent caractérisé par l'apparition de composantes hautes –fréquences au cours du mouvement basse fréquence de rotation. Sur la base d'un développement sur les modes basses fréquences, on observe que la transition se déplace au cours du mouvement de rotation jusqu'au décollement de bord d'attaque caractérisé par un fort pic de pression suivi d'oscillations basses fréquences.

Summary

In this paper, the wall pressure on the suction side of a hydrofoil undergoing a transient pitching motion of large amplitude is analysed experimentally. The obtained signals are of unsteady, turbulent wide-band, noisy, and involve various transient features of the flow that occur during the rotation. A novel signal processing method based on the Empirical Mode Decomposition (EMD) is tested. The EMD decomposes signals into frequency sub-band components called Intrinsic Mode functions (IMFs) by separating high frequency content of the signal from low frequency one. As a result, the EMD method allows to distinguish amongst noise several features of the flow such as the appearance of the boundary layer transition point accompanied by high frequency components during the low frequency transient motion. The transition point is first detected by the downstream transducers on the signal partially reconstructed using low frequency IMFs. It is observed to be moving toward the leading edge until boundary layer separation occurs characterized by a large pressure peak followed by low frequency oscillations.

I-INTRODUCTION

A work aimed to study an innovative cycloidal marine propulsion systems involving a hydrofoil in unsteady forced motion has been conducted by Benramdane et al. (2005). The performance prediction of such devices requires the knowledge of forces acting on lifting surfaces undergoing large amplitude forced motions leading to complex flow features including dynamic stall (Triantafyllou et al. 1993). This also involves the study of boundary layers in forced unsteady conditions, which is still a rather interrogative issue (Studer 2005) especially when transition, boundary layer separation, dynamic stall occur during the forced motion. The prediction of the instantaneous wall-pressure is fundamental in the analysis of the problem of flow induced forces and requires advances in experimental analysis techniques. Moreover, as the pressure at the wall is related to the vorticity, the understanding of wall-pressure fluctuations is of great importance to understand the dynamics of near-wall flow and particularly for unsteady flows. In this paper, the behavior of near-wall pressure signals of a hydrofoil's suction side undergoing a forced rotational motion with incoming flow is investigated. The proposed method based on the EMD, newly introduced by Huang et al. (1998), is used to detect transient phenomena in the pressure signals and allows to separate the pressure signal into different phases of interest such as laminar, turbulent and boundary layer separation phases. To this end, the original signal is decomposed into frequency sub-band components called Intrinsic Mode Functions (IMFs) from finer temporal scales to coarser ones using EMD.

II-EXPERIMENTAL SETUP

The experiments are carried out in the Ecole Navale's hydrodynamic tunnel, fitted with a 1m long and 0.192 m wide square cross test section shown in Figure 1. In this device, velocities of up to 15 m/s and pressures between 30 mbar and 3 bars can be achieved. The hydrofoil's relative maximum thickness is 12 % at 45% from the leading edge and the relative maximum camber is 2% at 50% from the leading edge. The chord length is c=0.150 m and the span is 0.191 m. More details can be found in Leroux (2003) or Leroux et al. (2005). The angle of incidence is given with respect to the zero angle of incidence. This latter is adjusted by aligning the foil chord to a free surface taken as a reference surface.

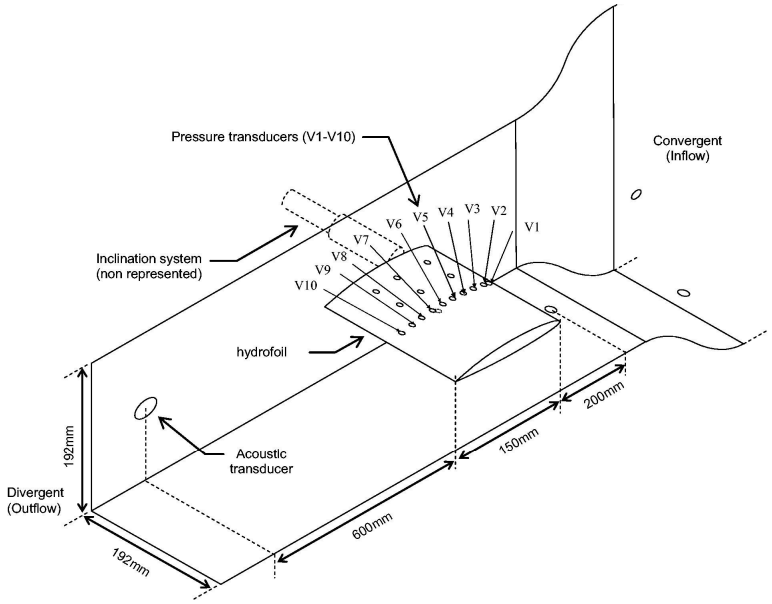

Fig. 1 Experimental set-up

Pressure measurements are carried out using seventeen piezoresistive transducers of 10 bars maximum pressure. The transducer locations labelled "V_i" are given in Figure 1. As shown,

one set of ten transducers is aligned along the chord on the suction side, starting from the leading edge at a reduced coordinate x/c=0.05 then from x/c=0.10 up to the trailing edge at coordinate x/c=0.90 with a step of 0.10 c. Two sets of three transducers are arranged parallel to this line in order to analyze three-dimensional effects, which is beyond the scope of this paper. The transducers responses are found to be linear in the range of interest. The pressure transducers are mounted into small cavities with a 0.5 mm diameter pinhole at the foil surface resulting in the Helmoltz natural frequency of the cavity of 85 kHz in water. There is a maximum frequency, f_c for which attenuation of the wall pressure spectrum occurs due to the spatial averaging over the surface of the transducer. From the transducers wavenumber response function, Lueptow (1993) showed that for a circular deflection transducer, an attenuation of -3 dB occurs for f_c = 0.88Uc/d where *Uc* is a typical convection velocity and d the diameter of the sensitive area of the transducer. Here considering d=0.5 mm (the pinhole diameter) and a convection velocity *Uc* of about 0.65×U (Farabee and Casarella (1991)) with a free stream velocity of *U* =8m/s, it is found that the theoretical cut off frequency is f_c =9152 Hz. Signals from the wall-pressure transducers are amplified and collected through a simultaneous sampling 16 channel, 16 bit A/D digitizer VXI HPE1432A, with a maximum available sample frequency of 51.2 kHz. The control parameters and the measurement data storage is performed by a PC through an HPE8491A/IEE1394 PC link.
For the experiments, the nominal free stream velocity U was 8 m/s, corresponding to a Reynolds number based on the foil chord length of 1.2×10^6. The hydrofoil rotates about an axis located at 25% about the leading edge from 0° to 14° at a constant rotational velocity of 1.4 °/s. The rotational speed of the stepping motor is set by the aid of a potentiometer that limits the frequency of excitation of the motor. Because of no angular position feedback during the test, the rotation speed is calculated from the recorded triggering signal of the stepper motor over the swept angle of rotation.

III-EMPIRICAL MODE DECOMPOSITION

In this paper a signal processing method based on the empirical mode decomposition (EMD) proposed by Huang et al. (1998) is used. The EMD is a full data driven algorithmic approach. The nonstationary signal is decomposed adaptively into intrinsic oscillatory components called intrinsic mode functions (IMFs) by means of an algorithm called sifting process. The basic principle of the method is to zero out IMFs which are likely to contain mostly noise while preserving the structure of the original signal. The basic principle is the extraction of intrinsic time scale components of the signal starting from finer temporal scales (high frequency modes) to coarser ones (low frequency modes). The total sum of the extracted IMFs matches the signal and therefore ensures signal complete reconstruction. Huang et al. (1998) have introduced the EMD method for analyzing data from nonstationary and nonlinear processes. This kind of processes are known to be hard to handle with classical signal processing tools such as wavelet analysis which is widely used in signals related to fluid mechanics which involve nonstationary and turbulent signals as reviewed by Farge (1992)

The EMD has found many applications in signal and image processing (Boudraa et al. 2004, Boudraa et al 2005, Cexus 2005), while it is beginning to be used in mechanical engineering (Gai 2006). The major advantage of the EMD is that the basis functions are derived from the signal itself, hence, the analysis is adaptive in contrast to the traditional methods where the basis functions are fixed such as in wavelet analysis.

In some sense the EMD can be seen as a type of wavelet decomposition whose sub-bands are built up as needed to separate the different components of a given signal *x(t)*. Each IMF replaces then the detail signals of *x(t)* at a certain scale or frequency band (Flandrin et al. 2004). The EMD picks out the highest frequency oscillation that remains in *x(t)*. Thus, locally, each IMF contains lower frequency oscillations than the one just extracted before and so it goes until we reach a signal that contains not enough oscillations to be extracted, the decomposition then stops and the obtained final signal is called the residue. The sifting algorithm involves the steps described in diagram of Figure 2:

1. The local minima and maxima of the input signal is estimated.
2. Upper and Lower envelopes are interpolated from local maxima, respectively minima using B-Spline method. Thus, the more the signal contains maxima and minima, the finer will be the first IMF, and the more will be the number of extracted IMFs.

3. Mean envelope is calculated.

4. Estimated IMF is calculated as the difference between input signal and mean envelope.

5. Estimated IMF is tested for stopping criterion satisfaction. If this latter is not satisfied, the sifting repeats with estimated *IMF* at this step as the input of the process.

The sifting is repeated several times (k) until the estimated *IMF* (h_k) satisfies the stopping criterion. The result of the sifting procedure is that $x(t)$ will be decomposed into a sum of $IMF_j(t)$, $j=1, \ldots n$ and a residual term $r_n(t)$

$$x(t) = \sum_{j=1}^{n} \mathrm{IMF}_j(t) + \mathrm{r}_n(t) \qquad (1)$$

Where n is the number of modes which is determined automatically using the stopping criterion. The stopping criterion is defined as the Standard Deviation (SD) computed from the two consecutive sifting results at iteration ($k-1$) and (k) as follows:

$$SD_k = \sum_{t=0}^{T} \frac{|h_{k-1}(t) - h_k(t)|^2}{h_{k-1}(t)^2} \qquad (2)$$

Where T is the total number of samples of input signal. Usually, SD is set between 0.2 to 0.3 (Huang et al. 1998).

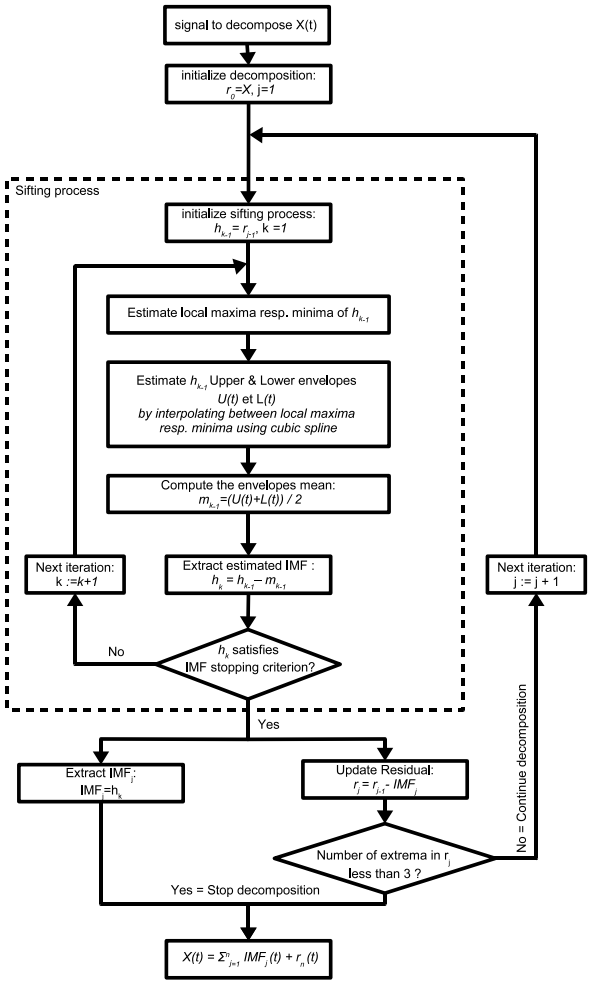

Figure 2 EMD algorithm

IV-RESULTS

The experience consists of driving the above described hydrofoil in rotational motion with a constant rotational speed value from 0° to 14°, corresponding to boundary layer separation. The acquisition of signals started 3s before rotation starts to end up at 20s. The obtained transient pressure signals are reported in Figure 3 for the transducers labelled "V2" to "V7" and "V10" located at reduced distances from the leading edge of x/c = 0.1, 0.2, 0.3, 0.4, 0.5, 0.6 and 0.9 respectively. Note that figure 3 is split into two parts (right and left) to allow visualization of details during the rotation motion. The wall pressure is shown in terms of temporal pressure coefficient defined by :

$$C_p(t) = \frac{P_{(t)} - P_{ref}}{0.5\rho U^2} \qquad (3)$$

With *P(t)* being the temporal pressure signals after calibration for each transducer (located at distance *x/c* from leading edge). And P_{ref} is the reference pressure measured from the transducer located on the bottom side of tunnel section, at distance 200 mm from the hydrofoil's leading edge (Figure 1) also used as the reference pressure for calibration and for flow control feedback. As shown several flow features occurs during the rotation motion depending on the transducer location. Except for transducer “V10” at *x/c*=0.9 near the trailing edge, the general trend is the continuous decrease of the pressure coefficient with the sudden occurrence of high frequency components (particularly for x/c = 0.1, 0.2, 0.3,) around 6 s, the fluctuations persist and increase during the rotation up to boundary layer separation occurring near the leading edge. As shown, the boundary layer separation is accompanied of very large fluctuations (right part of Figure 3).

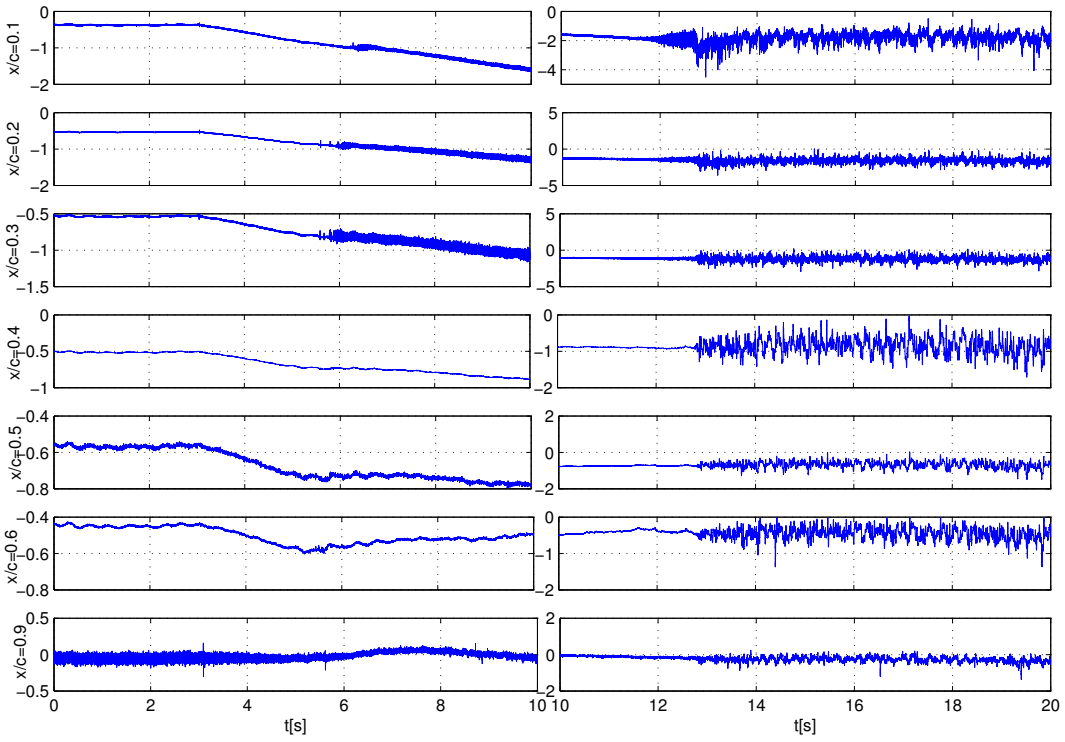

Figure 3 Cp(t) from transducers "V2" to "V7" and "V10" (from top to bottom). The signals are split in two parts (left and right).

The proposed method for signal decomposition relies on the idea of separating high frequency content of the flow from low frequency one. Indeed, as it is widely accepted, the power spectra of pressure fluctuations shows that most energetic structures of the pressure signal are concentrated on the lower frequency components and goes decreasing towards high frequency modes.

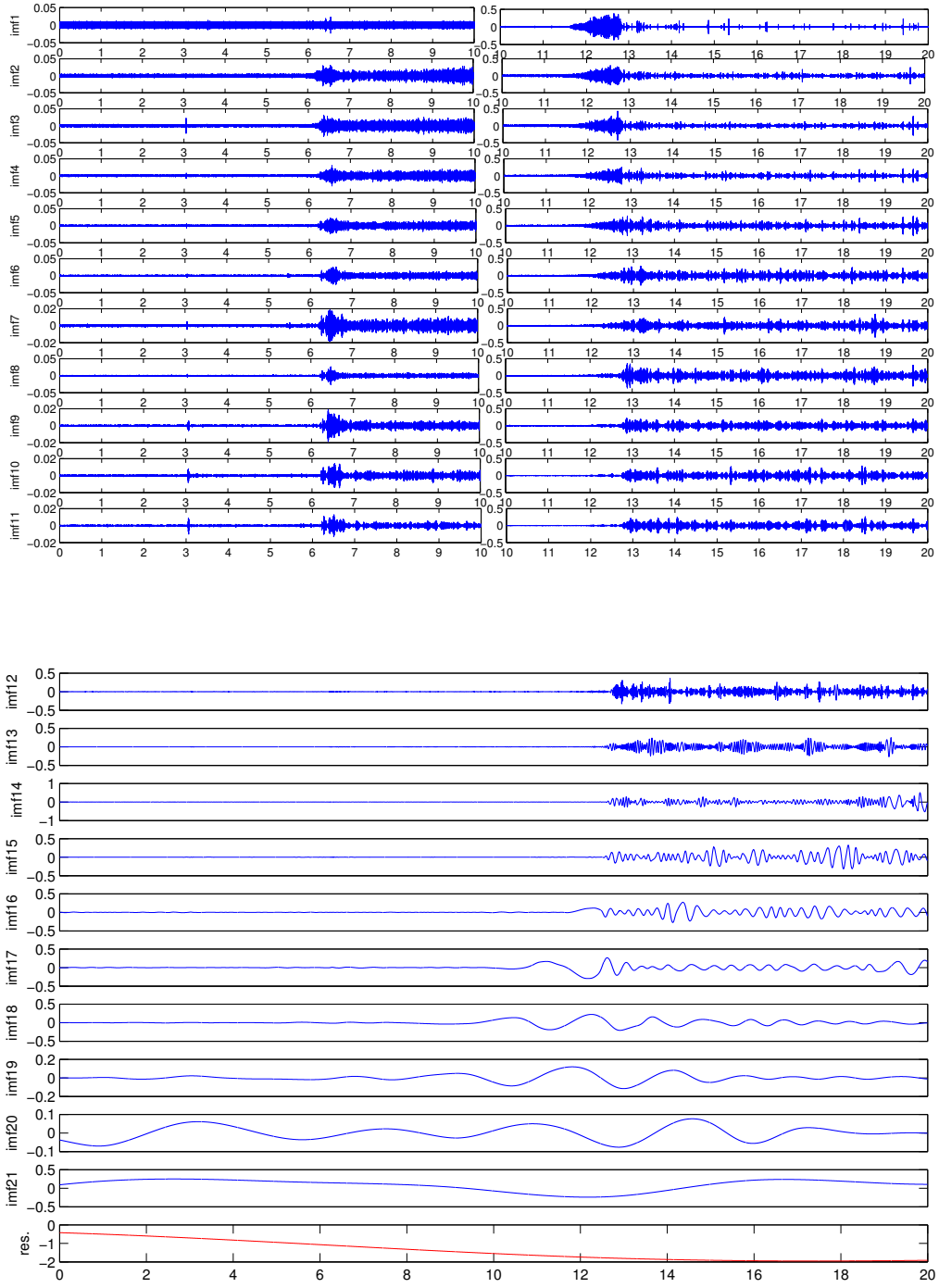

Figure 4 Empirical Mode Decomposition for wall-pressure signal of transducer "V2", x/c=0.1 in 21 IMFs. From high frequency IMFs (top) to low frequency IMFs , the last plot is the residue $r_n(t)$, n= 21. Note that for j=1 to 11, the IMFs are split in two parts.

Pressure coefficient signals are then processed using the EMD. As shown in Figure 4, EMD decomposition from transducer "V2" located near the leading edge (x/c=0.1) results in n=21 IMFs and a residue $r_n(t)$, the latter showing the monotone decrease of the pressure coefficient with no oscillation. Note that the plots for IMFs 1 to 11 are split in tow parts for a better visualization. This figure gives a very interesting pictures of how the frequency components appears during the transient motion. As shown, up to 6 s, no frequency is observable (except for IMF 1 that can be considered to be the environmental noise). It can be observed the high frequency activity occurring at about 6 s from IMF 2 to IMF 11. At nearly

the same time, it can be observed that two spots occur on IMF 1. A strong increase of high frequency activity occurs for IMF 1 to 4 (right part), just before the boundary layer separation around 12s -13 s, that is characterized by middle and low frequency activity (See IMF 16 to IMF 20 on the right part). IMF 20 showing very low frequency oscillation is attributed to low frequency variation of the free stream inflow due to the regulation system during measurements.

Thus, high frequency modes will be reconstructed separately from low frequency ones. IMF 1 is considered to be related to electronic environment noise, thus it will not be considered for signal reconstruction. The rest of high frequency IMFs probably contain noise as well, but they also retain signal of high frequency spectra of the flow. Although signal to noise ratio is hard to estimate in such case, these IMFs will be accounted for in signal reconstruction to avoid loss of information of high frequency nature which is of prime interest as far as transient phenomena are concerned.

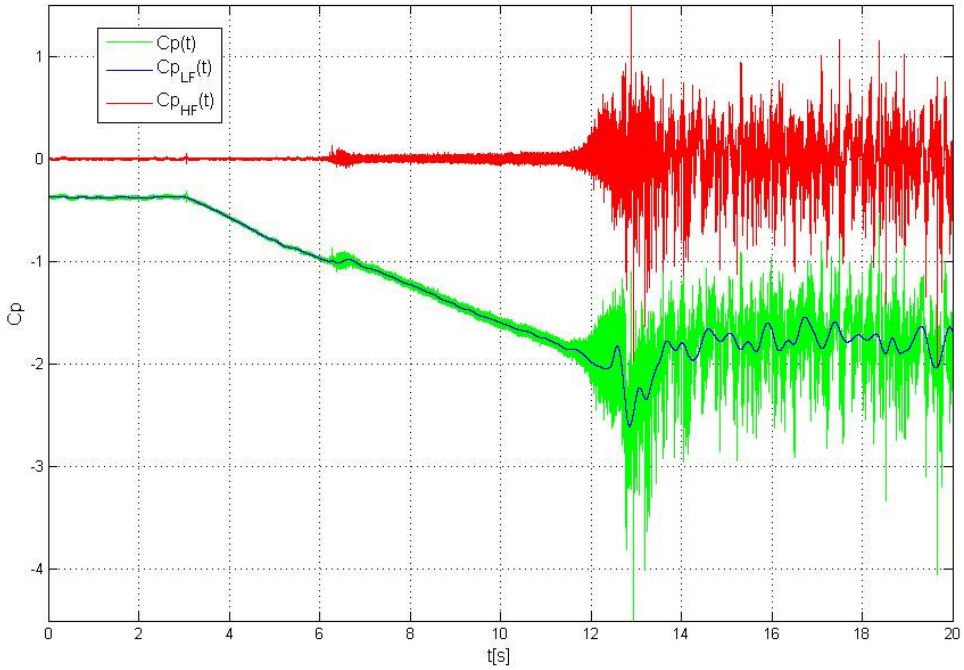

Figure 5 Pressure coefficient Cp(t) à x/c=0.1 (transducer "V2") during foil rotation. Direct signal, Low Frequency Reconstruction and High Frequency Reconstruction (see Eq. 4)

Pressure coefficient signals are then reconstructed for each transducer from "*n-k*" selected IMFs of low frequency modes including the residue that represent the overall trend of the signal and contain the Low Frequency part of the signal energy. Let us call these signals, the low frequency EMD-filtered pressure coefficient, $Cp_{LF}(t)$. The "k-1" IMFs are summed to construct the higher frequency fluctuations of the pressure coefficient. This component will be called High Frequency EMD-filtered pressure coefficient $Cp_{HF}(t)$. These two components are given by:

$$\begin{cases} Cp_{LF}(t) = \sum_{j=k+1}^{n} IMF_j(t) + \mathrm{r}_n(t) \\ Cp_{HF}(t) = \sum_{j=2}^{k} IMF_j(t) \end{cases} \quad (4)$$

A typical representation can be seen in Figure 5 for transducer "V2" with k=15 showing the direct signal, the low frequency decomposition and the high frequency decomposition. As

shown, the LF modes depict the global smooth trend of the pressure coefficient whereas the HF modes show the high frequency activity of wall-pressure fluctuations during the foil transient rotation.

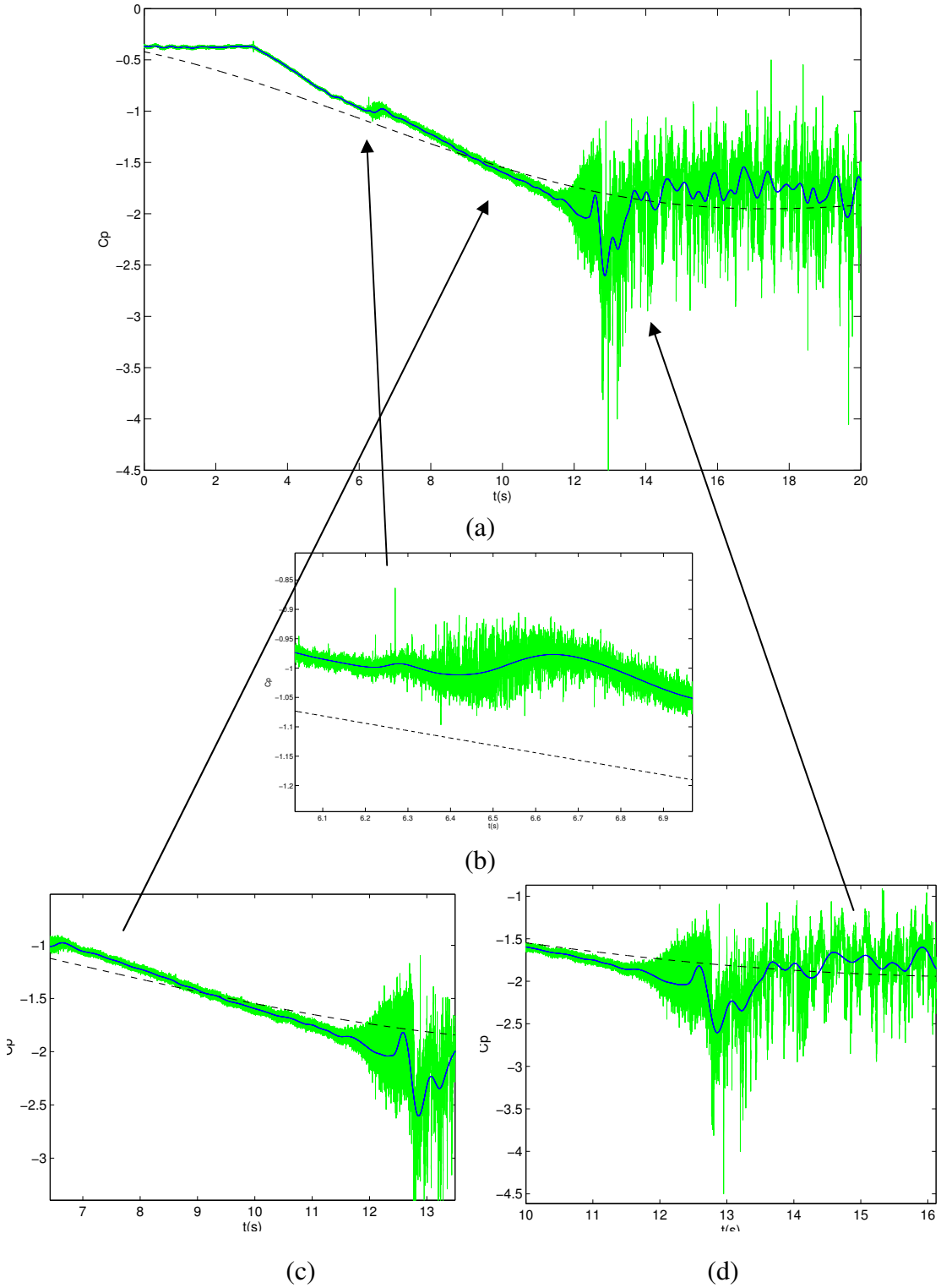

Figure 6 Rough pressure signal for "V2" and Low Frequency EMD Decomposition with the five lowest frequencies IMFs + $r_n(t)$ (See Equ. 4). The dashed line is $r_n(t)$. (a) Total signal during foil rotation, (b) Phase 2 : transition, (c) Phase 3 : turbulent, (d) Phase 4: Boundary Layer separation

Figure 6 show that the pressure coefficient evolution can be separated in five distinct phases.
Phase 1, from 3 s to 6.3 s (See Figure 6.a): the pressure coefficient signal decreases linearly along with the hydrofoil's rotation with very small fluctuations.

Phase 2, from 6.3 s to 6.8 s (Figure 6.b): The pressure coefficient show a plateau behaviour with a low frequency oscillation resulting in two distinct bumps (clearly showed by the LF decomposition) together with an increase of high frequency fluctuations. It is interesting to observe that a kind of spots appear on IMFs 1-4 (Fig 4). This phenomenon reveals the development of a laminar bubble separation (experimentally observed) at the leading edge together with the transition occurrence downstream.

Phase 3, from 6.8 s to 11.5 s (Figure 6.c):. The fluctuations persist and are more pronounced than that of the previous phase, the flow is fully turbulent.

Phase 4, from 11.5 s to 15.07 s (Figure 6.d). At this stage, it is interesting to observe that the mean pressure remains rather constant from 11.5s to 12.8s and the amplitude of the high frequency fluctuations increases strongly. This is clearly shown on Figure 4 for IMF number 1 to 4 (on the right side). At 12.8s, a strong pressure drop occurs resulting of boundary layer separation at the leading edge.

Phase 5, at 15.07 s, the hydrofoil's rotation is stopped. It can be observed that the pressure signal increases gradually to recover a constant mean value with large pressure fluctuations due to vortex shedding from the leading edge. This is observed to be quasi-periodic but with large amplitude modulation. The frequency modulation can be clearly observed on IMF number 15, 16 and 17 on Figure 4.

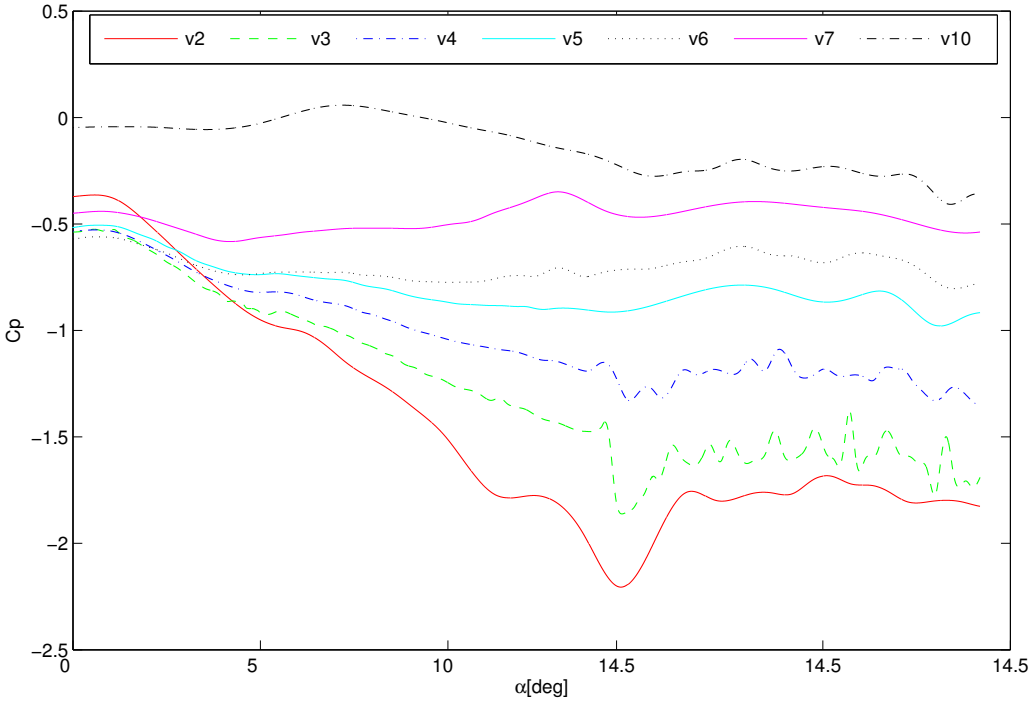

Figure 7 C_{PLF} (α (t)) during foil rotation, k=15 see Eq.4

It is interesting to describe the spatial evolution of the pressure coefficient along the foil chord. For instance, Figure 7 represents the Low Frequency EMD-filtered pressure coefficients along the chord at various angles of incidence during the foil rotation. Several points can be observed. The plateau behaviour around 5° resulting of a boundary layer bubble separation development near the leading edge is observable on all the transducers except for

transducers “V10” near the trailing edge that records an increase of the pressure during the same time. It was observed that the plateau occurs first on the downstream transducers than moves towards the leading edge moves towards the leading edge A plateau is observable again around 11° just before separation occurs. The pressure drop around 14.5° corresponding to boundary separation is clearly observed up to x/c=0.3 (Transducer “V3”).

Comparison can also be done between static state pressure coefficient (Cp(x/c) at a fixed angle of incidence obtained from measurements for static hydrofoil conditions. Results are plotted in Figure 8. From this figure, it can be observed that in relatively low speed transient motion of the hydrofoil, the pressure coefficient is globally slightly over the static state one.

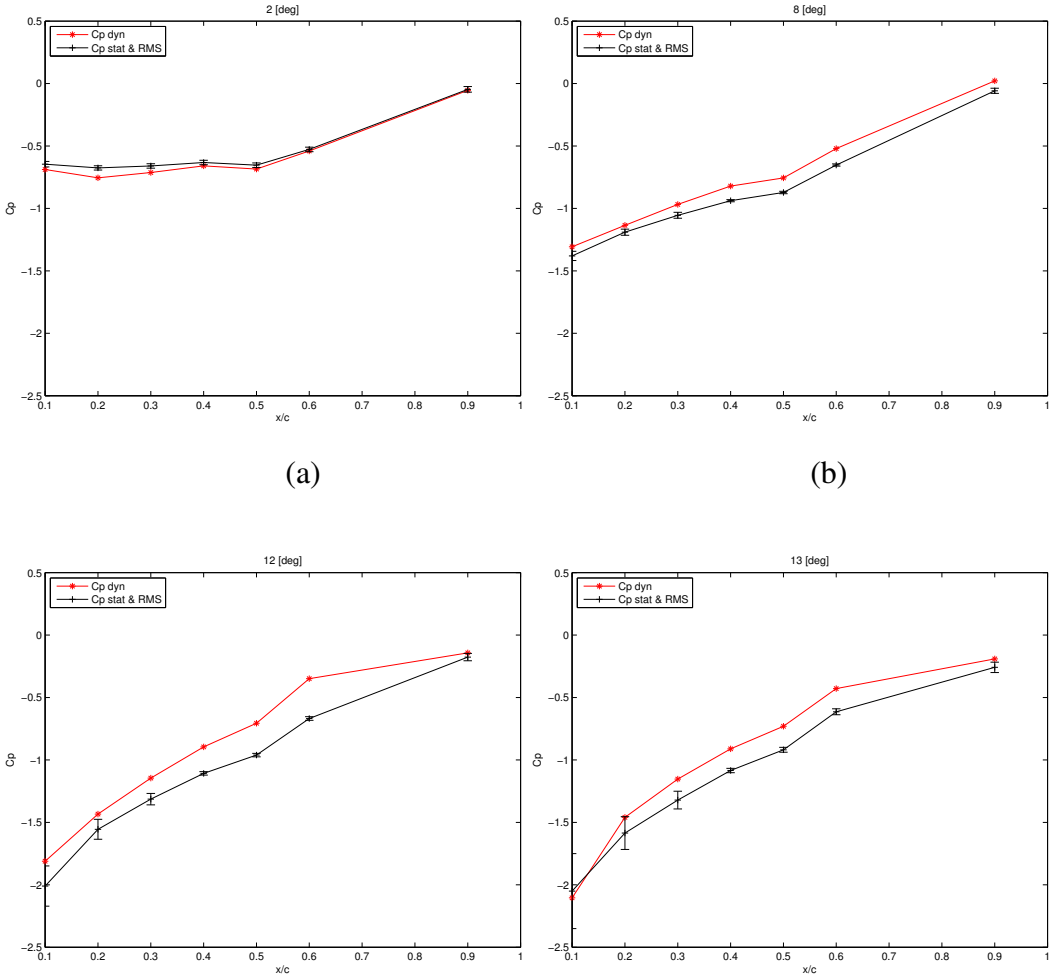

Figure 8 Cp_{LF} (x/c) and static Cp(x/c) at angles of 2° (a), 8° (b), 12° (c) and 13°(d). Vertical bars correspond to fluctuation intensity in the static case.

The obtained EMD-filtered signals along the foil chord allow us to construct a transient chordwise pressure coefficient for both low $C_{pLF}(x/c, t)$ and high $C_{pHF}(x/c, t)$ frequency modes and to follow their evolution in time during the rotation of the hydrofoil.

Fig. 9 shows the spatio-temporal evolution of the low frequency pressure coefficient $C_{pLF}(x/c, t)$. This representation is relevant for showing conserved history of the evolution in time. We can clearly see the separation bubble and transition occurrence near the leading edge the pressure drop at boundary layer separation and the associated low frequency oscillation. High frequency modes being reconstructed separately into what we called fluctuating value

will be considered for further analysis.

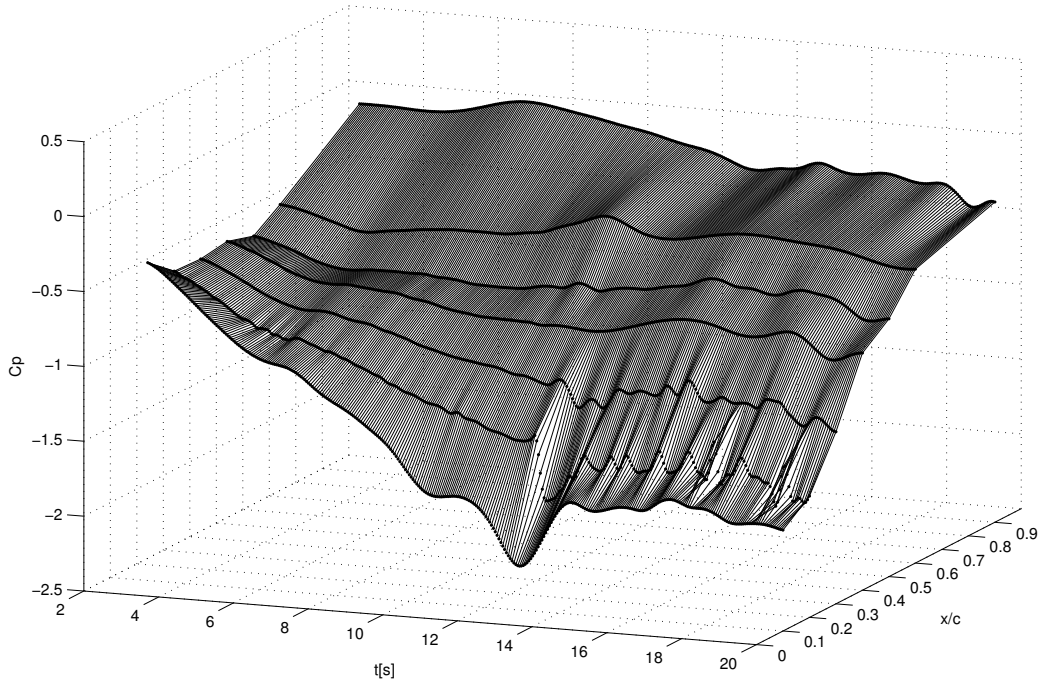

Figure 9 Spatio-temporal evolution of the low frequency EMD wall-pressure coefficient $C_{pLF}(x/c,t)$ during foil rotation

V-CONCLUSIONS

In the present work we investigated the near-wall pressure signals of a hydrofoil in transient motion up to boundary layer separation. The analysis uses a novel method based on the EMD technique consisting of decomposing the signal into basic intrinsic functions (IMF). This method is found to be well suited for typical transient hydrodynamic signals which are usually unsteady, wide-band, noisy, and turbulent. This analysis showed how the transition to turbulence appears on pressure signals. Comparison between transducer signals in the chordwise direction also showed that this transition point is moving upstream until boundary layer separation occurs. Further work is in progress to develop further analysis particularly about the spectral contents of each IMF and time-frequency analysis.

VI-REFERENCES

Benramdane S, Damay T,Hauville F, Deniset F & Astolfi J.A, 2005. flow Study on a Hydrofoil undergoing forced motions: application to cycloidal propulsion. 10e Journe de l'Hydrodynamique, pp 39-52.

Boudraa A-O., Cexus J.C., Salzenstein F. & Guillon L., "IFestimation using empirical mode decomposition and nonlinear Teager energy operator,"Proc. IEEE ISCCSP, pp. 45-48, 2004.

Boudraa A.O., Pollet C., Cexus J.C. & Saidi Z., "Caracterisation des fonds marins par d´ecomposition modale empirique" 20`eme Colloque sur le Traitement du Signal et de l'Image (GRETSI), Louvain-La-Neuve, Belgium, 6-9, september, 2005.

Cexus J.C, 2005, Nonstationnary signal processing using Huang transform, Teager-Kaiser energy operator and Huang- Teager transform (THT). PhD Thesis, Universit´e RENNES 1.

Farabee T. H. and Casarella M. J., 1991, "Spectral features of wall pressure fluctuations beneath turbulent boudary layers", Physics of Fluids A 3 (10), October 1991, pp 2410-2420.

Flandrin P., Rilling G. & Goncalves P., ”Empirical Mode Decomposition as a Filter Bank,” IEEE Sig. Proc. Lett., vol. 11, no. 2, pp. 112-114, 2004.

Gai G., 2006, ”The processing of rotor startup signals based on empirical mode decomposition”. Mechanical Systems and Signal Processing 20(2006), pp. 222-235

Huang N.E., Shen Z., Long S.R., Wu M.C., Shin H.H., Zheng Q., Yen N.C., Tung C.C. and Liu H.H., 1998 ”The Empirical Mode Decomposition and the Hilbert spectrum for nonlinear and non-stationary time series analysis,” Proc. Royal Soc. London A, vol. 454, pp. 903-995, 1998.

Leroux J.B, 2003, Experimental study of partial cavitation instabilities on Hydrofoil in water tunnel by instantaneous wall pressure measurements. PhD Thesis, Ecole Centrale Nantes/ Universite de Nantes.

Leroux J.-B. , Coutier-Delgosha O., Astolfi J. A. 2005“A Joint Experimental and Numerical Study of Mechanisms Associated to Instability of Partial Cavitation on Two-Dimensional Hydrofoil”. Physics of Fluids, 17,1 2005.

Lueptow, R.M, 1993, Wall Pressure Transducer Spatial Resolution, NCA-Vol. 15. 168, Flow Noise Modeling, Measurement, and Control, ASME 1993, pp. 49-55.

Studer G, 2005, Experimental and numerical study of laminarturbulent transition in unsteady flow. PhD Thesis, Ecole nationale supérieure de l’aéronautique et de l’espace.

Triantafyllou G.S, Triantafyllou M.S, Grosenbaugh M.A, 1993, Optimal Thrust development in oscillating foils with application to fish propulsion. J. Fluid. Struct. 7(2):205-224